Supporting Information

Cuprous Oxide Based Chemiresistive Electronic Nose for Volatile Organic Compounds Discrimination

Baishu Liu,[†] Xue Wu,[†] Kenneth WL Kam,[⊥] Wai-Fung Cheung,[⊥] Bo Zheng[†]*

[†]Department of Chemistry, The Chinese University of Hong Kong, Shatin, N.T., Hong Kong, China

[⊥]Qi Diagnostics Limited, Mongkok, Kowloon, Hong Kong, China

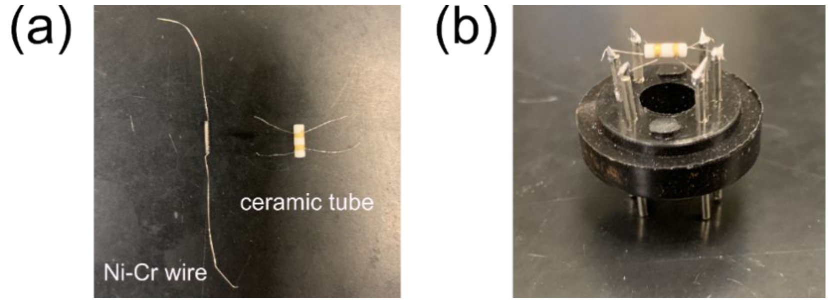

Figure S1. (a) Photograph of the Ni-Cr wire and the ceramic tube. (b) Photograph of the gas sensor.

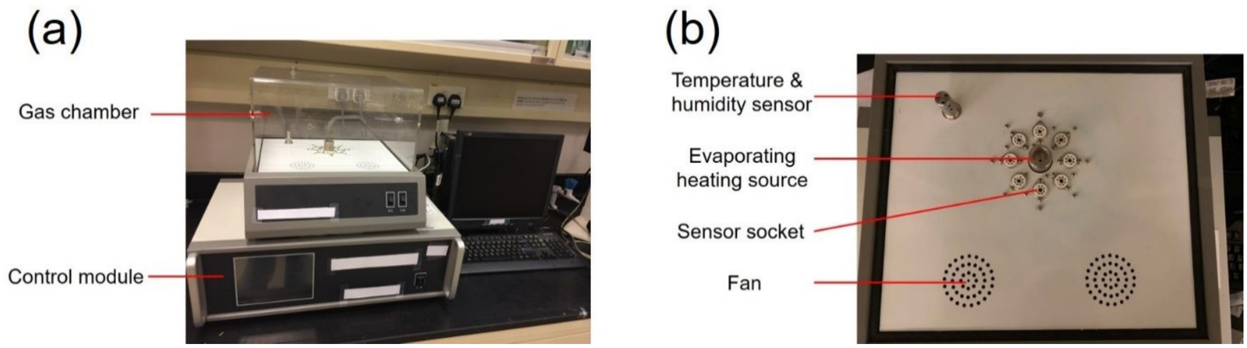

Figure S2. (a) Photograph of the gas analysis system CGS-8. (b) Sensor panel of the gas analysis system CGS-8.

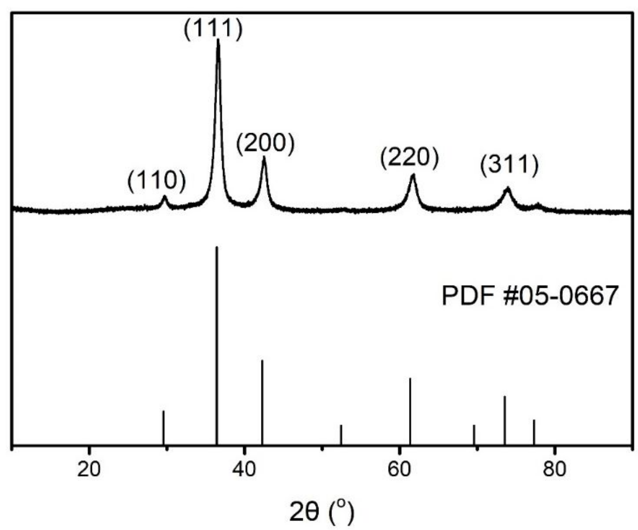

Figure S3. XRD pattern of Cu_2O nanospheres (top) and the standard XRD pattern of Cu_2O (PDF #05-0667, bottom)

Table S1. Chemical structures of the organosilanes.

Name	Chemical structure	Corresponding abbreviation of the silanized Cu_2O
PAPTMS	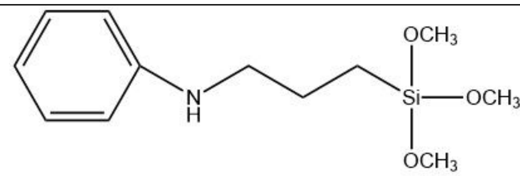	PA-Cu_2O
APTMS	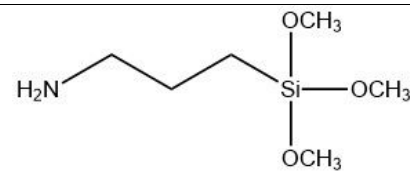	AP-Cu_2O
MAPTMS	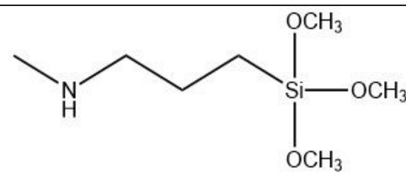	MA-Cu_2O
CPTMS	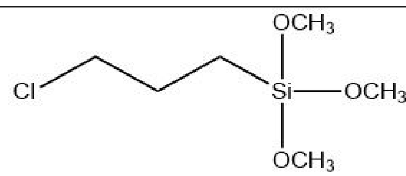	CP-Cu_2O
PTES	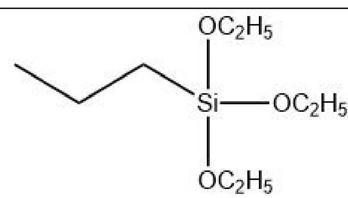	P-Cu_2O

Table S2. Zeta potentials of Cu_2O and the organosilane functionalized Cu_2O nanospheres.

The functionalized Cu_2O	Zeta potential (mV)
Cu_2O	34.2
PA-Cu_2O	26.9

AP-Cu_2O	172.7
MA-Cu_2O	61.6
CP-Cu_2O	-23.6
P-Cu_2O	30.5

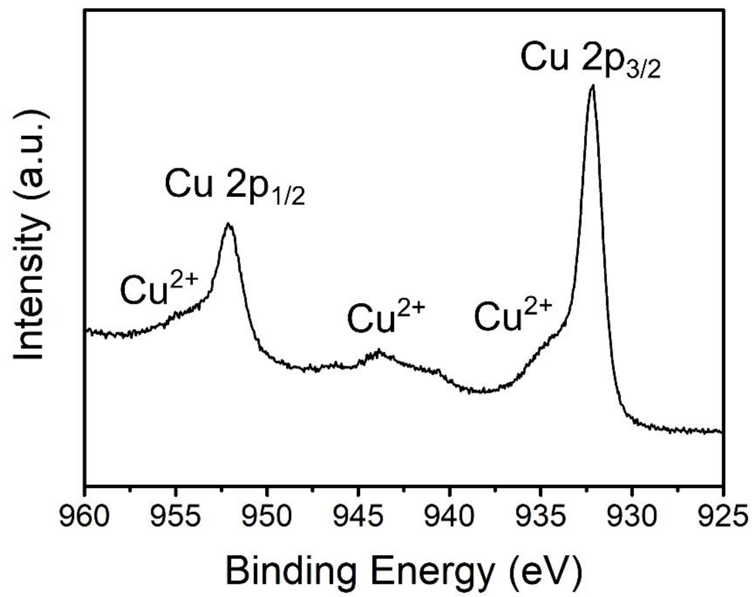

Figure S4. XPS Cu 2p spectrum of P-Cu_2O.

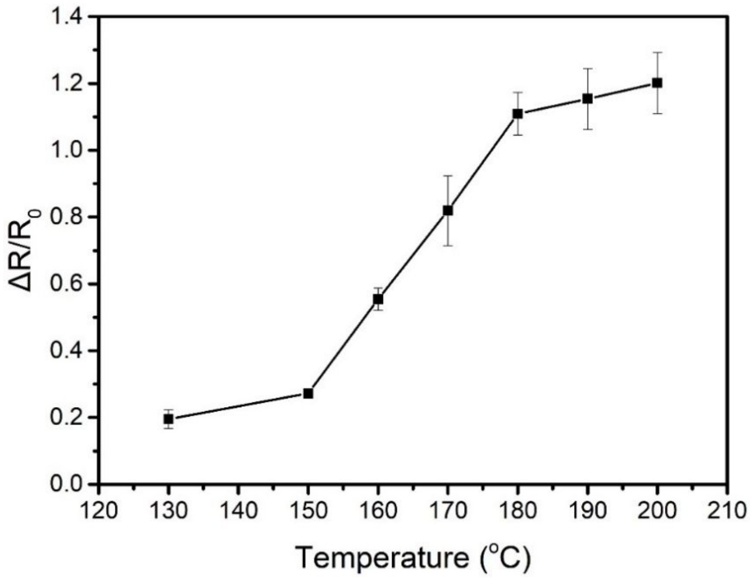

Figure S5. Resistance response of P-Cu_2O to 25 ppm ethanol at the operating temperature of 130-200 ^{o}C.

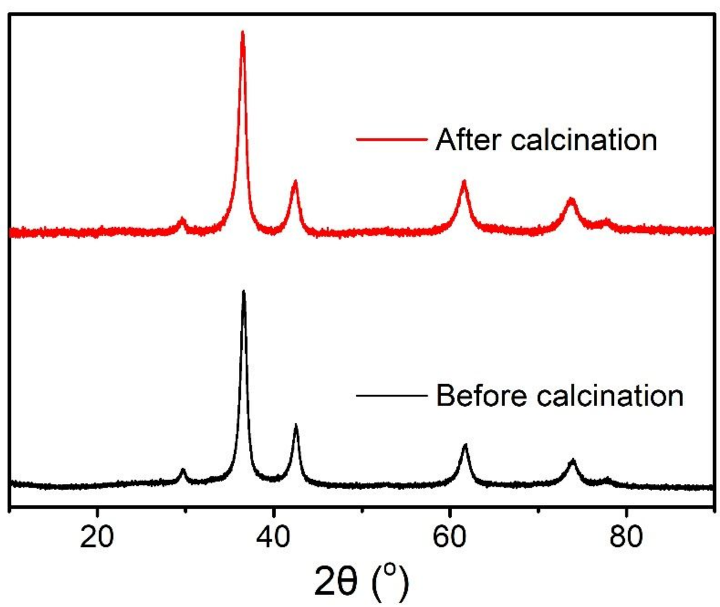

Figure S6. XRD patterns of Cu_2O nanospheres before and after calcination at 180 ^{o}C for 1 hour.

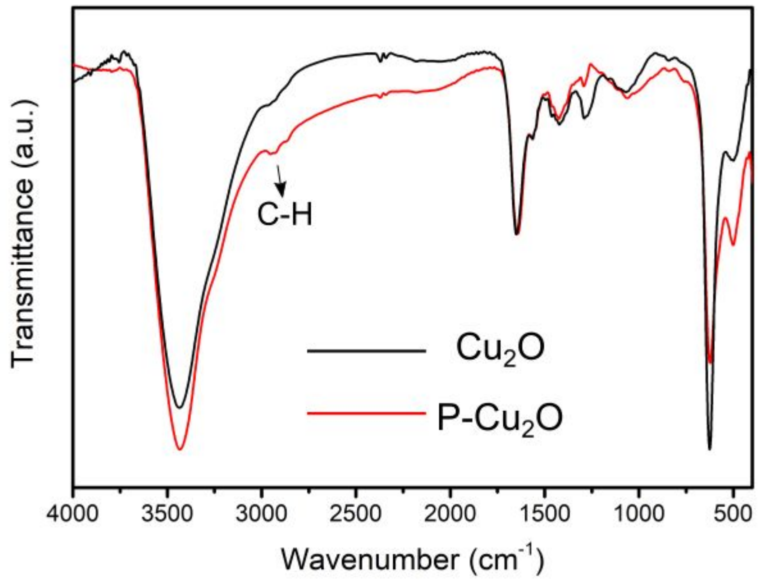

Figure S7. FT-IR spectra of Cu_2O and P-Cu_2O nanospheres after calcination at 180 ^{o}C for 1 hour.

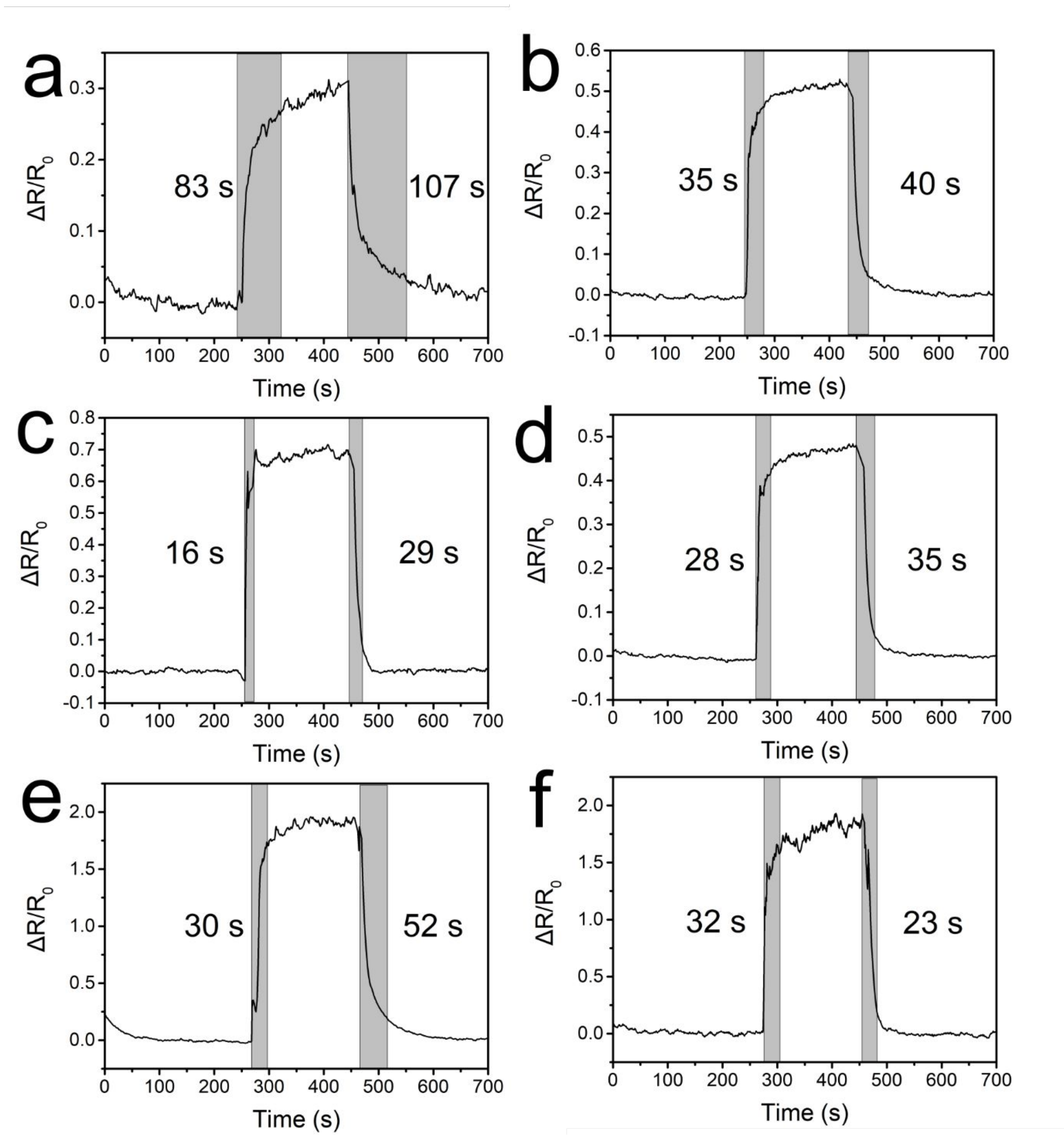

Figure S8. Response and recovery curves of the sensor units upon the exposure to 50 ppm ethanol. (a) Cu_2O; (b) PA-Cu_2O; (c) AP-Cu_2O; (d) MA-Cu_2O; (e) CP-Cu_2O; (f) P-Cu_2O.

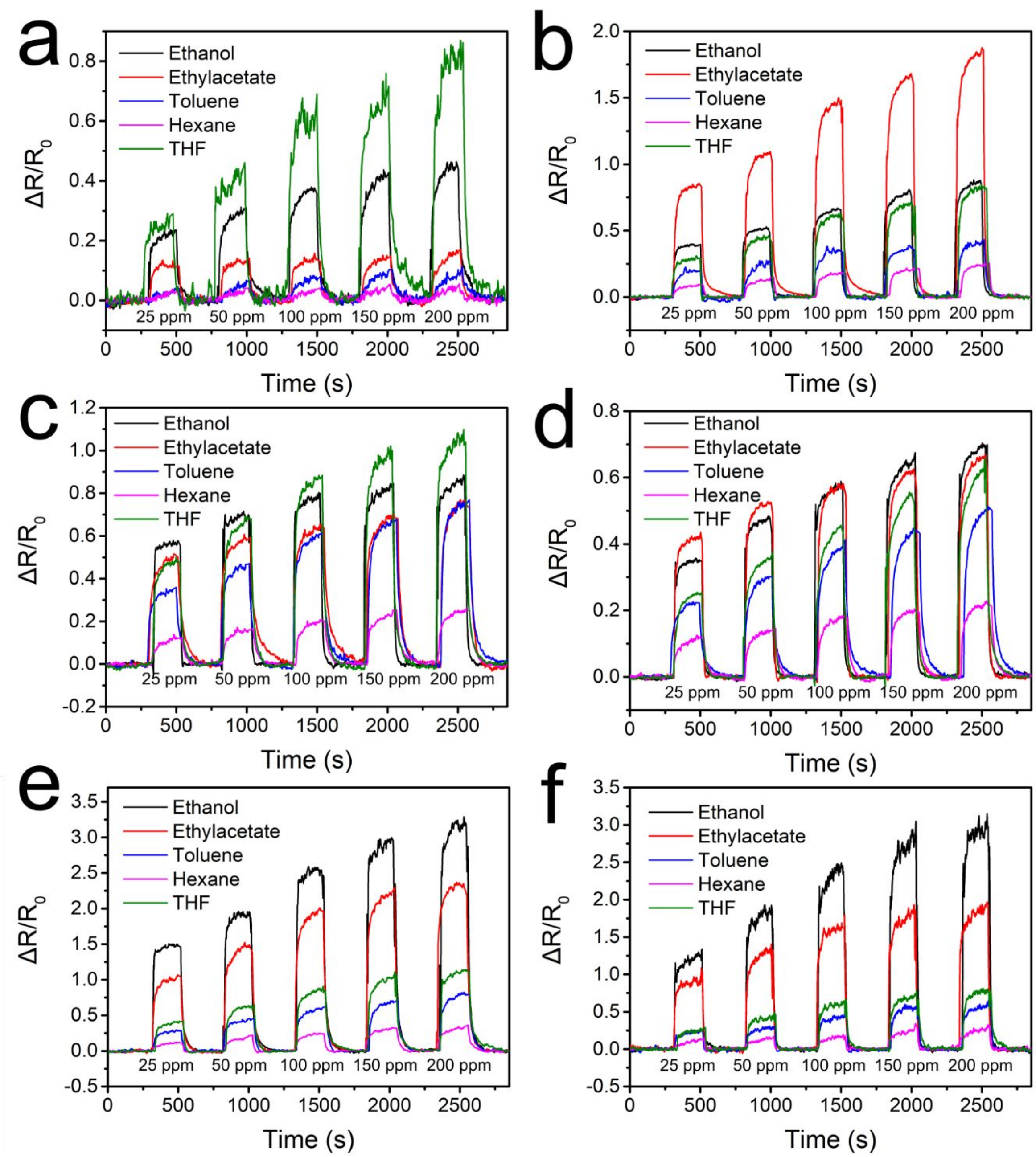

Figure S9. Real-time resistance responses of Cu_2O and five functionalized Cu_2O nanospheres upon the exposure to 25-200 ppm model VOCs. (a) Cu_2O; (b) PA-Cu_2O; (c) AP-Cu_2O; (d) MA-Cu_2O; (e) CP-Cu_2O; (f) P-Cu_2O.

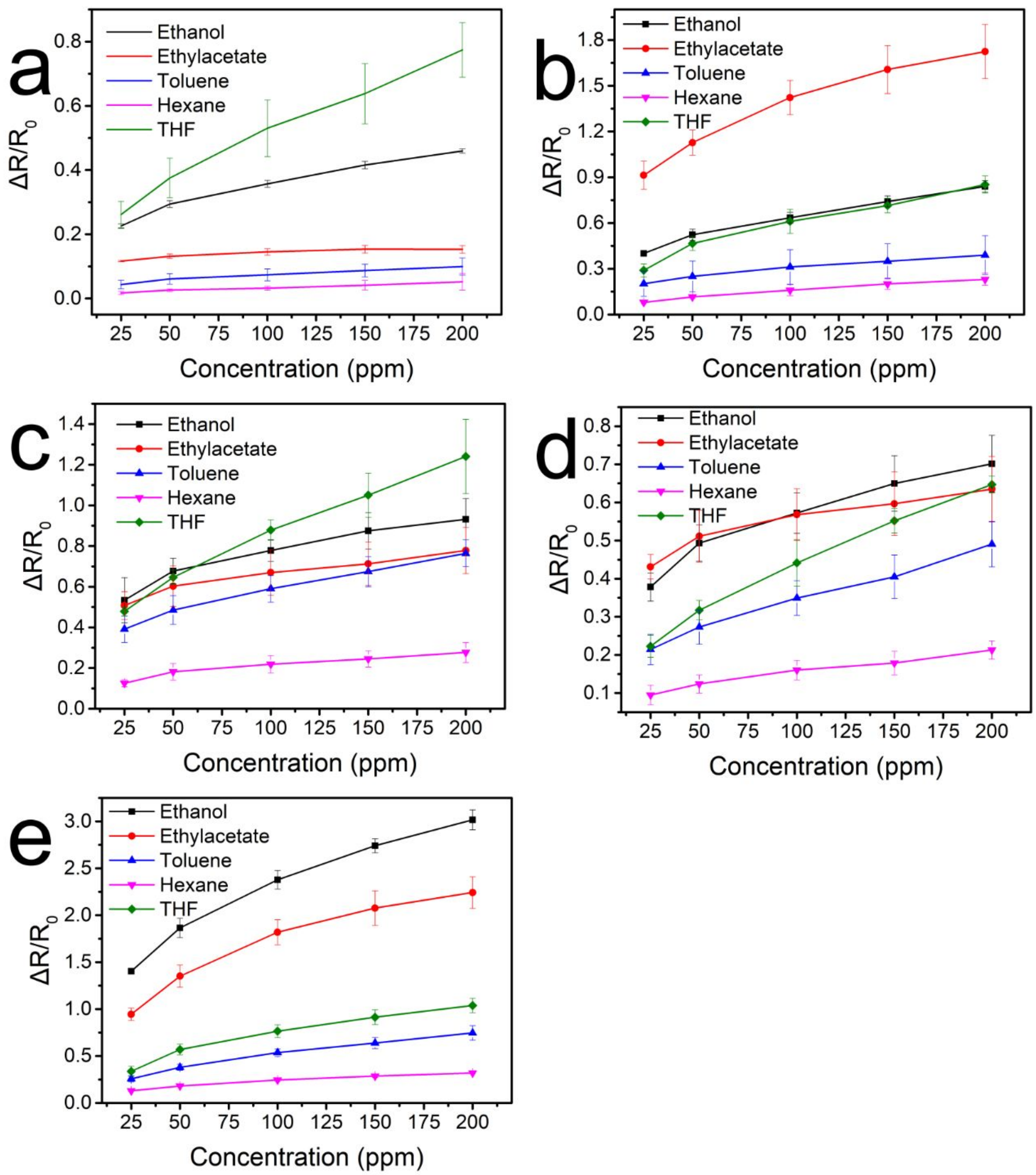

Figure S10. Resistance responses of Cu_2O and four functionalized Cu_2O nanospheres upon the exposure to 25-200 ppm model VOCs. (a) Cu_2O; (b) PA-Cu_2O; (c) AP-Cu_2O; (d) MA-Cu_2O; (e) CP-Cu_2O.

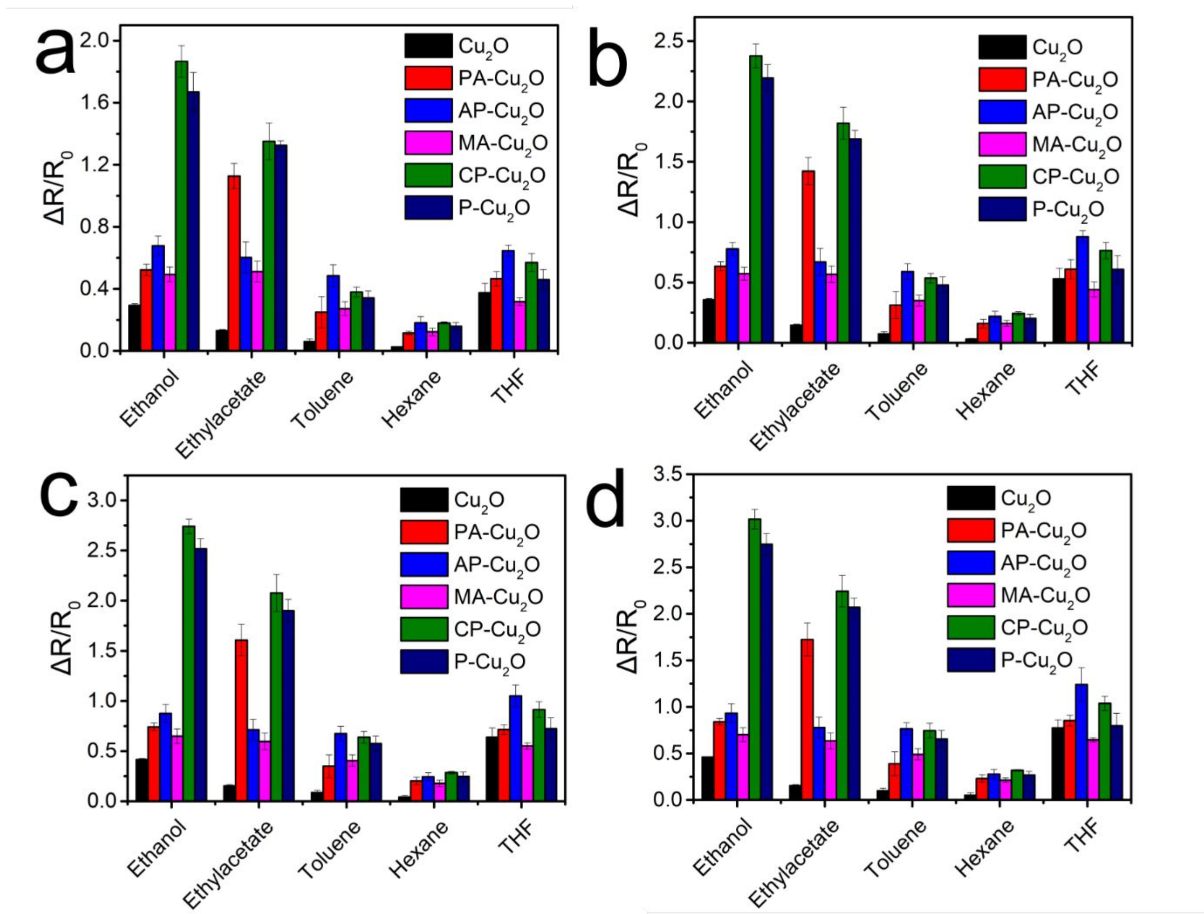

Figure S11. Resistance responses from the sensor units upon the exposure to the model VOCs. (a) 50 ppm; (b) 100 ppm; (c) 150 ppm; (d) 200 ppm.

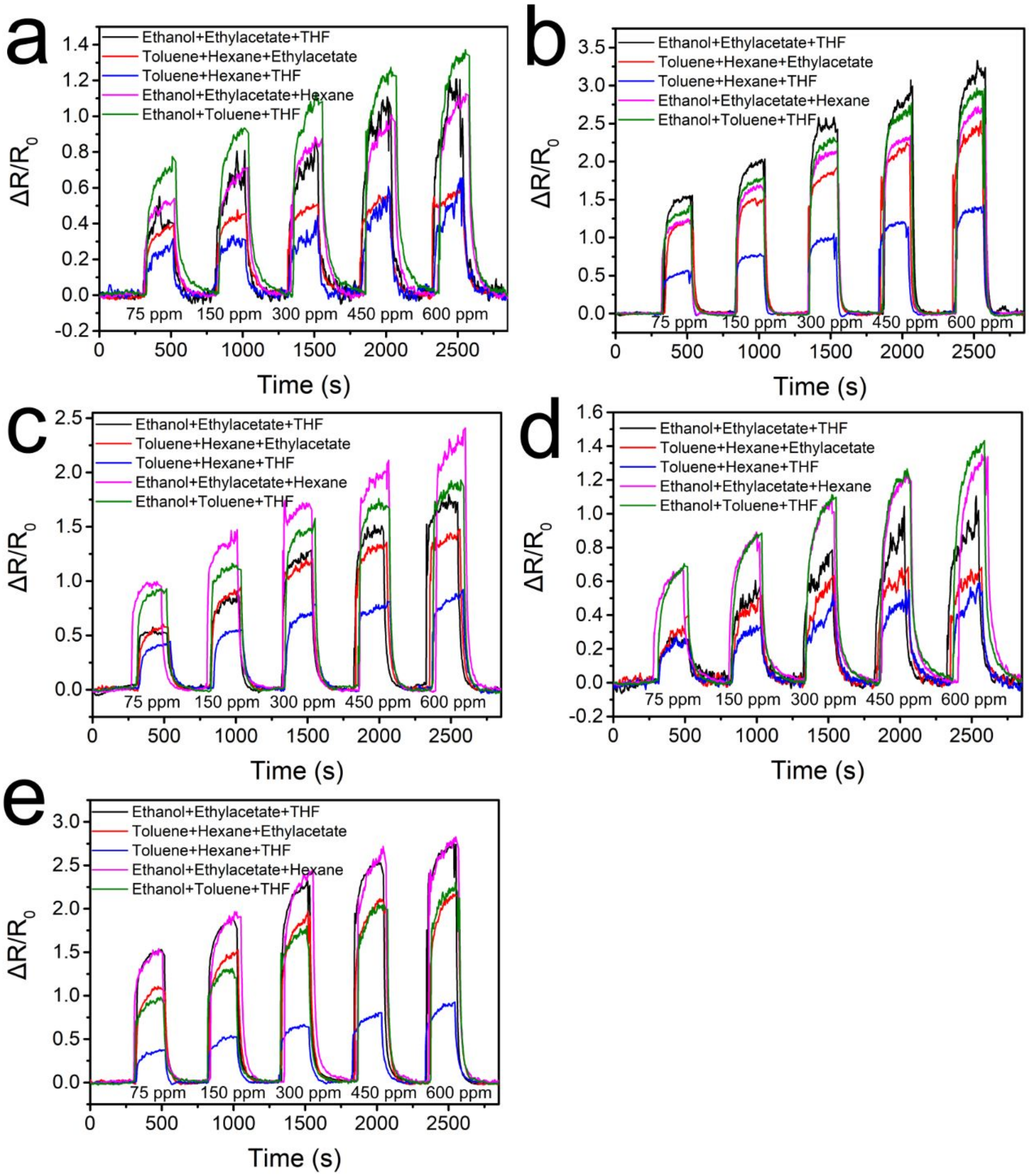

Figure S12. Real-time resistance responses of Cu_2O and four functionalized Cu_2O nanospheres upon the exposure to 75-600 ppm ternary VOC mixtures. (a) Cu_2O; (b) PA-Cu_2O; (c) AP-Cu_2O; (d) MA-Cu_2O; (e) CP-Cu_2O.

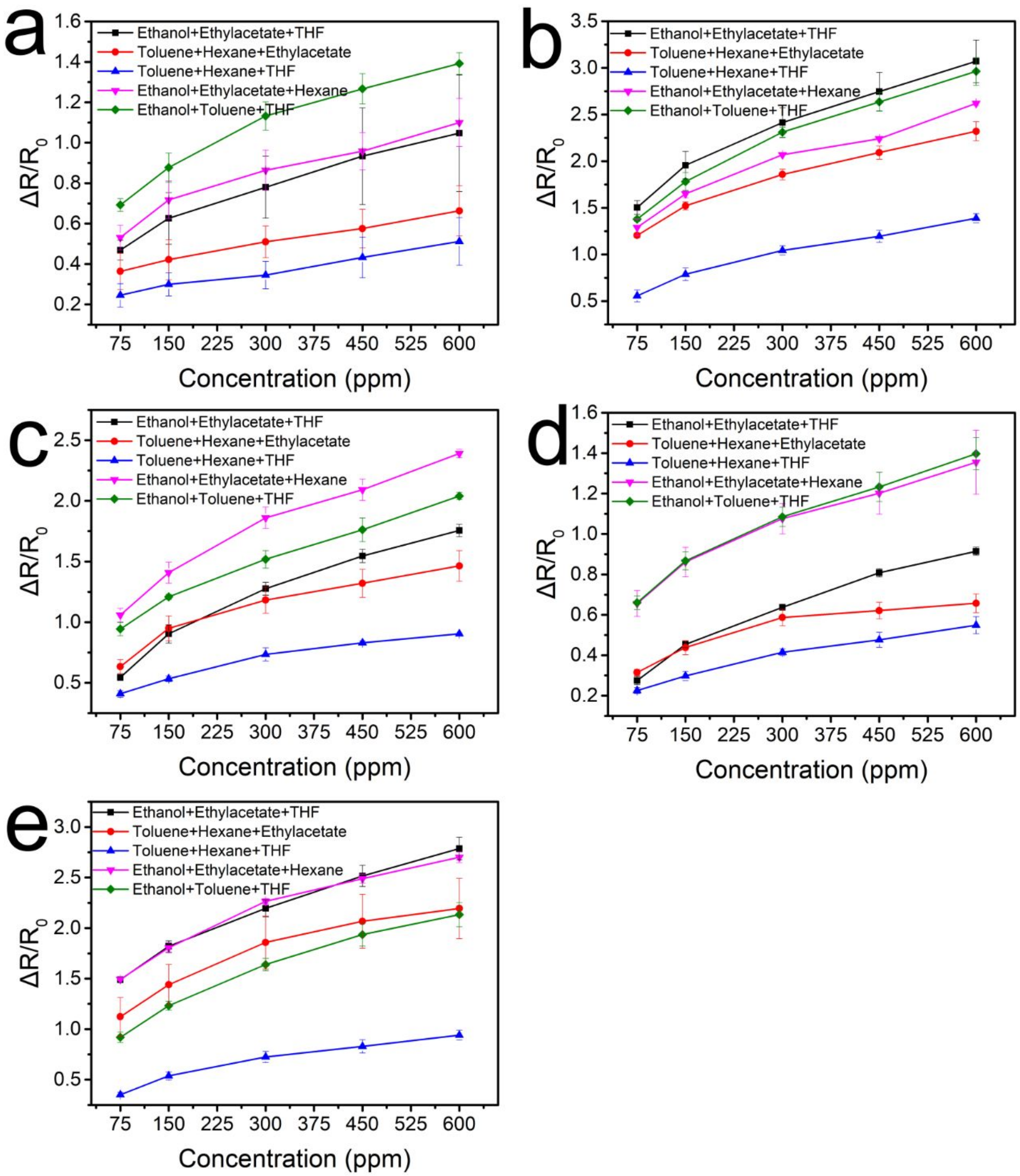

Figure S13. Resistance responses of Cu_2O and four functionalized Cu_2O nanospheres upon the exposure to 75-600 ppm ternary VOC mixtures. (a) Cu_2O; (b) PA-Cu_2O; (c) AP-Cu_2O; (d) MA-Cu_2O; (e) CP-Cu_2O.

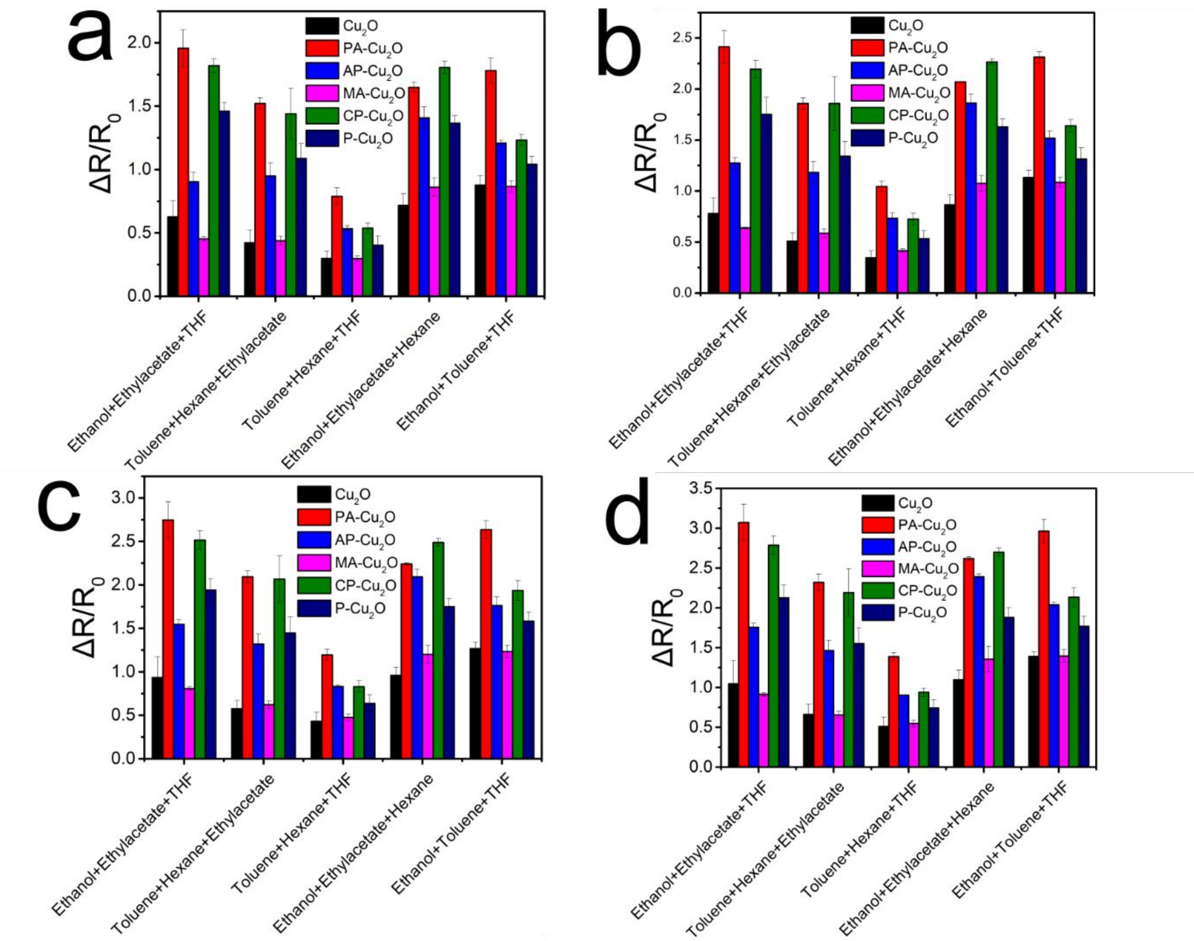

Figure S14. Resistance responses from the sensor units upon the exposure to ternary VOC mixtures. (a) 150 ppm; (b) 300 ppm; (c) 450 ppm; (d) 600 ppm.

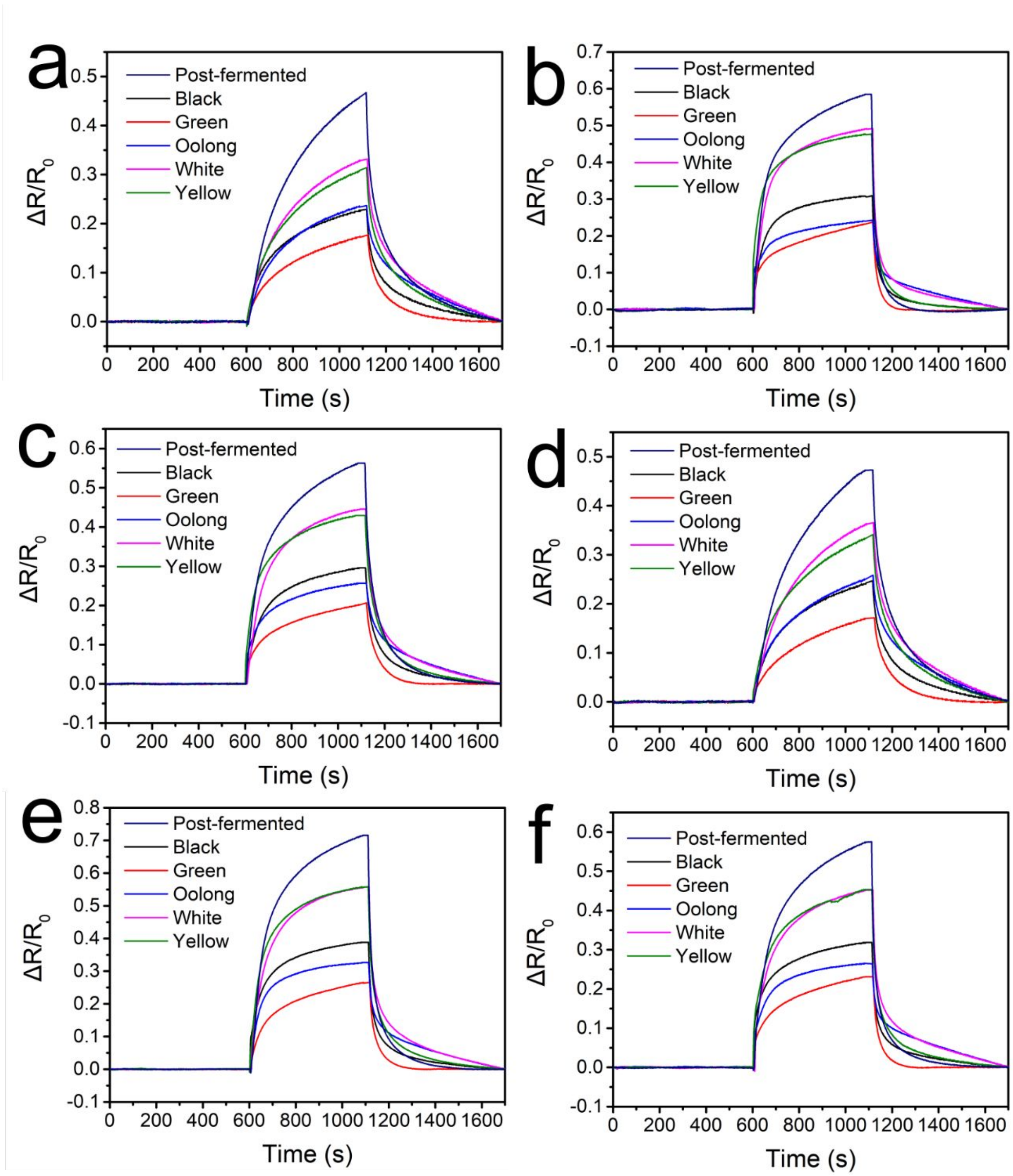

Figure S15. Real time resistance responses of Cu_2O and five functionalized Cu_2O nanospheres upon the exposure to six types of tea leaves. (a) Cu_2O; (b) PA-Cu_2O; (c) AP-Cu_2O; (d) MA-Cu_2O; (e) CP-Cu_2O; (f) P-Cu_2O.